

## Localized parallel electric fields associated with inertial Alfvén waves

R. E. Ergun

*Department of Astrophysical and Planetary Sciences, University of Colorado, Boulder, Colorado 80309-0391 and Laboratory for Atmospheric and Space Physics, University of Colorado, Boulder, Colorado 80303*

L. Andersson and Y.-J. Su

*The Laboratory for Atmospheric and Space Physics, University of Colorado, Boulder, Colorado 80303*

D. L. Newman and M. V. Goldman

*Center for Integrated Plasma Studies, University of Colorado, Boulder, Colorado 80309*

W. Lotko

*Dartmouth College, Hanover, New Hampshire 03755*

C. C. Chaston and C. W. Carlson

*Space Sciences Laboratory, University of California, Berkeley, California 94720-7304*

(Received 10 November 2004; accepted 1 April 2005; published online 20 June 2005)

Measurements of intense, localized parallel electric fields are reported in association with inertial Alfvén waves and accelerated electron fluxes in a space plasma. The parallel electric fields are localized to several hundreds of Debye lengths and carry potentials on the order of the energy of the accelerated electron fluxes. The structures are observed at sharp maxima or minima of the perturbation magnetic field of the Alfvén wave, indicating high shear or rapid changes in the parallel current but near-zero, large-scale parallel currents. The localized electric-field structures are not entirely consistent with published double-layer models or observations in the aurora and may represent a new class of parallel electric-field structures or double layer, which are an important feature of the nonlinear evolution of Alfvén waves and of the electron acceleration processes. These data also represent a possible example of cross-scale coupling from Alfvén wavelengths to Debye scales. © 2005 American Institute of Physics. [DOI: 10.1063/1.1924495]

### I. INTRODUCTION

The Alfvén wave is one of three principal modes that govern the lowest-order dynamics of many laboratory, space, and astrophysical plasmas. At small perpendicular scales, the shear Alfvén wave is also capable of electron acceleration.<sup>1–3</sup> Space physics and astrophysical examples include some of the most intense auroral arcs at Earth,<sup>4–7</sup> the Io–Jupiter interaction,<sup>8–10</sup> the solar corona<sup>11,12</sup> (and references therein), and extragalactic jets.<sup>13</sup> Small-scale Alfvén waves recently have been the focus of laboratory studies.<sup>14,15</sup> The linear damping process of kinetic Alfvén waves has been well documented,<sup>16</sup> but the nonlinear process of particle heating and acceleration is not well understood.

In the case of the aurora, it was recognized<sup>2</sup> that particle acceleration by Alfvén waves could occur in the near-Earth plasma, where  $\beta < m_e/m_i$  (the electron-to-ion mass ratio). In this low- $\beta$  environment, the ion gyroradius is smaller than the electron skin depth ( $\delta_e = c/\omega_{pe}$ , where  $\omega_{pe}$  is the electron plasma frequency). The “inertial” Alfvén waves develop a finite parallel electric field ( $E_{\parallel}$ ) if the perpendicular wave number ( $k_{\perp}$ ) is on the order of  $\delta_e$ . It has been established that inertial Alfvén waves accelerate electrons in the polar cusp region<sup>6</sup> and in a class of intense, dynamic auroral displays associated with substorm expansions.<sup>17,18</sup> The electron fluxes accelerated through this process are strongly field-aligned and extend over a broad energy range. They are distinct from the electron fluxes from quasistatic parallel electric fields

(e.g., Ref. 19), which have a broad angular distribution, but are confined to a narrow energy range.

The complexity of the Alfvén wave–electron acceleration problem is greatly increased by the fact that the plasma density and magnetic field dramatically change between the magnetosphere and the ionosphere on a distance scale that is less than the Alfvén wavelengths. The inhomogeneous medium not only strongly modifies a propagating Alfvén wave, but can partially trap a relatively narrow frequency band ( $\sim 0.1$ – $1$  Hz) between the conductive layer in the ionosphere (at  $\sim 100$ – $300$  km in altitude) and the peak in Alfvén speed at  $\sim 1 R_E$ . This region has been designated as the “ionospheric resonator.”<sup>20</sup>

Test particle simulations (not self-consistent) have demonstrated that observed field-aligned electron fluxes are consistent with acceleration by inertial Alfvén waves.<sup>21</sup> There are two basic acceleration mechanisms. Under certain ionospheric conditions, the Alfvén wave can trap electrons, which are observed as a field-aligned population with particle velocities up to twice the local Alfvén speed.<sup>22</sup> The wave also can accelerate electrons through a resonant process. These electrons escape the wave as it slows down in the high-density ionosphere. This population is observed with energy and pitch angle dispersion as a result of the magnetic-field topology and the travel distance between the point they were released by the wave and the observation.<sup>22</sup>

The test particle simulations, however, often employ inertial Alfvén waves with very large  $k_{\perp}$  and very large

$\Delta\mathbf{B}(E_{\perp})$  to develop a small but significant parallel electric field ( $E_{\parallel}$ ) in the simulation. Alfvén waves observed in association with electron acceleration can have smaller amplitudes in  $\Delta\mathbf{B}(E_{\perp})$  and smaller  $k_{\perp}$ . The linear value of  $E_{\parallel}$  predicted by theory and in simulations is less than 1 mV/m and cannot be observed with current satellite instrumentation (under the best conditions, parallel electric fields are measured to an accuracy of a few mV/m). The wave potential in the simulations often needs to exceed the electron temperatures to reproduce the observed electron fluxes. Such large potentials are expected to lead to a variety of nonlinear behaviors<sup>23–26</sup> that, as of yet, have not been fully explored. Furthermore, none of the linear studies have successfully described the anti-earthward electron acceleration that is commonly observed with Alfvén waves.

The purpose of this article is to present observational evidence of localized, large-amplitude parallel electric fields associated with inertial Alfvén waves in the auroral region. Previous observations<sup>27–29</sup> and some theoretical studies<sup>23–26</sup> suggest that nonlinear processes play an important role in enhancing the electron acceleration by Alfvén waves. Both observations and simulations show Alfvén waves with a triangular shape in the magnetic-field signal suggesting strong current shear and spiky parallel electric fields with amplitudes much larger than what is predicted by linear theories. The scale size of the parallel electric fields are several hundreds of Debye lengths ( $\lambda_D \sim 1\text{--}10$  m), well separated from the Alfvén wavelength ( $\sim 10\,000$  km) indicating a highly localized, nonlinear dissipative process energized by a larger-scale Alfvén wave.

## II. OBSERVATIONS

Figure 1 presents observations from the Fast Auroral SnapshoT (FAST) satellite.<sup>30–32</sup> The satellite is  $\sim 2960$  km in altitude, crossing the near-midnight auroral zone from south to north in the northern hemisphere. The horizontal axis is 10 s of time during which the satellite traversed  $\sim 50$  km to the north. A summary of the plasma parameters is given in Table I.

The top panel, Fig. 1(a), displays the measured  $E_{\parallel}$  filtered to dc  $\text{--}200$ -Hz frequency band. A description of the validation of parallel electric-field measurements has been previously published,<sup>33,34</sup> so only a brief description is provided here.  $E_{\parallel}$  is calculated from the dot product of the vector electric field ( $\mathbf{E}$ ) (derived from four probes that form a tetrahedron) and the measured magnetic field ( $\mathbf{B}$ ) in the rotating frame of the spacecraft. In Fig. 1(a), the trace represents the quantity  $\mathbf{E} \cdot \mathbf{B} / |\mathbf{B}|$ . The accuracy of  $E_{\parallel}$  in Fig. 1(a) is approximately  $\pm 50$  mV/m. Thus, many of the features in  $E_{\parallel}$  may be due to density perturbations or cross talk from the perpendicular electric fields. The large-amplitude (roughly 100 mV/m) spikes at  $\sim 9:42:42.5$  UT and  $\sim 19:42:46.0$  UT (indicated by dashed lines), however, are interpreted as valid parallel electric fields (positive is earthward in the northern hemisphere).

Figure 1(b) plots  $E_{\perp}$ , the dc electric field perpendicular to  $\mathbf{B}$  and in the direction closest to the spacecraft velocity (positive is mostly northward and nearly parallel to the sat-

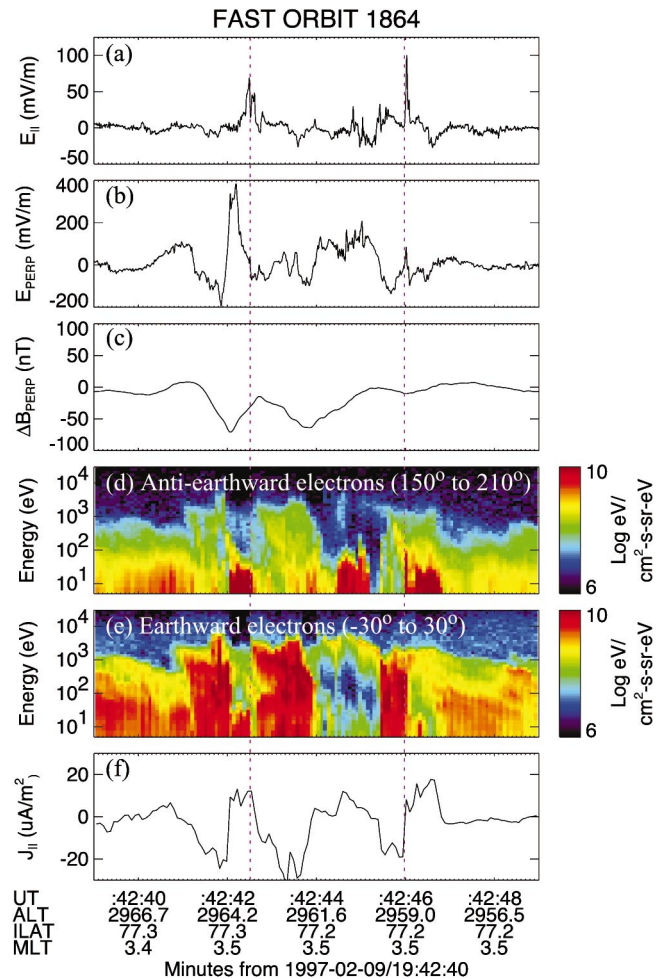


FIG. 1. (Color). Observation of a large-amplitude parallel electric field associated with an inertial Alfvén wave. (a)  $E_{\parallel}$  at 200-Hz bandwidth. (b)  $E_{\perp}$  at 200-Hz bandwidth. The component is closest to the spacecraft velocity. (c)  $\Delta B_{\perp}$ , the measured magnetic field minus the Earth's model field, at  $\sim 5$ -Hz frequency band. (d) Anti-earthward ( $150^{\circ}$ – $210^{\circ}$  in pitch angle) electron energy flux vs energy and time at 79-ms resolution. (e) Earthward ( $-30^{\circ}$ – $30^{\circ}$  in pitch angle) electron energy flux vs energy and time at 79-ms resolution. (f) The field-aligned current derived from 5-eV to 30-keV electron fluxes.

ellite's velocity). Figure 1(c),  $\Delta B_{\perp}$ , displays the magnetic field minus the Earth's model field in the dc to  $\sim 5$ -Hz frequency range. The displayed component is perpendicular to the model  $\mathbf{B}$  and  $E_{\perp}$  in Fig. 1(b). Figures 1(d) and 1(e) display, respectively, the anti-earthward and earthward electron energy fluxes as a function of energy and time. Figure 1(f) displays the field-aligned current derived from the measured electron energy fluxes in the 5-eV–30-keV energy range.

Figures 1(b)–1(e) represent an often observed signature of electron acceleration by an inertial Alfvén wave.<sup>4–6,18–21</sup>  $\Delta B_{\perp}$  appears to have roughly three cycles at  $\sim 2$ -s period (as measured by a moving spacecraft), consistent with the period of the Alfvén resonator.<sup>20</sup> It is possible, however, that the 2-s period is dominated by Doppler shift, in which case the perpendicular wavelength is roughly 10 km (the spacecraft is moving at  $\sim 6$  km/s). In this example,  $\Delta B_{\perp}$  also has a triangle-shaped wave form.  $E_{\perp}$  displays far more structure than  $\Delta B_{\perp}$ , indicating an electrostatic component that results

TABLE I. Plasma, Alfvén wave, and  $E_{\parallel}$  parameters for Fig. 1.

Plasma parameters	Estimated value	Alfvén wave	Estimated value	$E_{\parallel}$ structure	Estimated value
$n_e$	$\sim 100 \pm 50 \text{ cm}^{-3}$	$\lambda_{\perp}$	$> 10 \text{ km}$	Velocity	20 km/s
$T_e$	$\sim 20 \text{ eV}^a$	$\lambda_{\parallel}$	$\sim 10^4 \text{ km}$	Potential	100 V
$\delta_e = c / \omega_{pe}$	$\sim 10 \text{ km}$	$f$	$\sim 0.5 \text{ Hz}$	Size	1 km
$ \mathbf{B}  / (\mu_o \rho)^{1/2}$	$\sim 10\,000 \text{ km/s}$	$ \mathbf{E}  /  \Delta \mathbf{B} $	4000 km/s		
$1 / (\Sigma_p \mu_o)$	$\sim 100 \text{ km/s}$				

<sup>a</sup>Non-Maxwellian plasma.

from small perpendicular scales. These latter two features are indications that the Alfvén wave is nonlinearly evolving.

The direction of the electron fluxes correspond to the slope of  $\Delta \mathbf{B}_{\perp}$ . Anti-earthward electron fluxes, Fig. 1(d), occur with a positive slope in  $\Delta \mathbf{B}_{\perp}$ , whereas earthward electron fluxes, Fig. 1(e), are seen with a negative slope. The electron fluxes in both directions display velocity dispersion, whereby the higher energy fluxes arrive before lower energy fluxes. The field-aligned current ( $J_{\parallel}$ ) derived from the energetic (5 eV–30 keV) electron fluxes has a “square” wave appearance, which is concordant with the triangle shape in the magnetic field. The field-aligned currents have rapid changes (if interpreted as temporal structure) or high shear (if interpreted as spatial structure).

The ratio  $E_{\perp} / \Delta \mathbf{B}_{\perp} \sim 4000 \text{ km/s}$  using the 2-s period harmonics of the signals. This ratio is approximately a factor of 5 lower than the local Alfvén speed ( $v_A \sim 10^4 \text{ km/s}$ ) and about a factor of 10 higher than the ratio expected for static fields ( $1 / \mu_o \Sigma_p \sim 100 \text{ km/s}$ , where  $\Sigma_p \sim 5 \Omega^{-1}$  is the estimated height-integrated Pedersen conductivity). The observations indicate a partial standing wave.

The large-amplitude signals in  $E_{\parallel}$  are observed as the electron fluxes are in transition from anti-earthward to earthward in the first event, and earthward to anti-earthward in the second event. The direction of  $E_{\parallel}$  (earthward in both cases) is such that it accelerates electrons anti-earthward. Prior to the events, velocity-dispersed electrons indicate that the primary acceleration is far from the spacecraft.

A magnified view of the second parallel electric-field structure ( $\sim 19:42:46.0 \text{ UT}$ ) and the electron fluxes is displayed in Fig. 2. The top panel, Fig. 2(a), is identical to Fig. 1(a) except for the time scale. Figures 2(b) and 2(c) display the anti-earthward and earthward electron fluxes at  $\sim 2$ -ms resolution at five separate energies labeled on the plot. One can see that the  $E_{\parallel}$  structure occurs in the transition region/time, whereby the earthward electron fluxes are decreasing and the anti-earthward electron fluxes are increasing. At the position/time of the spiky  $E_{\parallel}$  structure, both directions of field-aligned fluxes are present. Velocity dispersion in the electron fluxes prior to the event is marked with dashed arcs. The source of these fluxes is calculated to come from between 125 and 250 km earthward of the spacecraft. The dispersive pattern is indicative of a wave-resonant acceleration process.<sup>21</sup>

The speed of the  $E_{\parallel}$  structure is estimated at 20 km/s ( $\pm$  a factor of 2) along  $\mathbf{B}$  from time delays between probes on the electric-field instrument. A speed of  $\sim 20 \text{ km/s}$ , roughly

the ion acoustic speed, would yield  $\sim 100 \text{ V}$  potential and is in consort with the enhanced fluxes of  $\sim 75 \text{ eV}$  electrons that are coincident with the parallel electric field [Fig. 2(b)]. At 20 km/s, the size of the structure is  $\sim 1 \text{ km}$ , roughly several hundred  $\lambda_D$ . The  $E_{\parallel}$  structure (anti-earthward electric field) is observed with strong earthward electron fluxes, which appear to be moderately perturbed. The ambient field-aligned current is near zero (reversing from anti-earthward to earthward), so the  $E_{\parallel}$  structure is not entirely consistent with the current-carrying double layers observed in the static upward and downward current regions of the aurora.<sup>33–38</sup> The speed of the  $E_{\parallel}$  structure ( $\sim 20 \text{ km/s}$ ) is well separated from the Alfvén speed ( $\sim 10\,000 \text{ km/s}$ ), so it is clearly transient and formed locally.

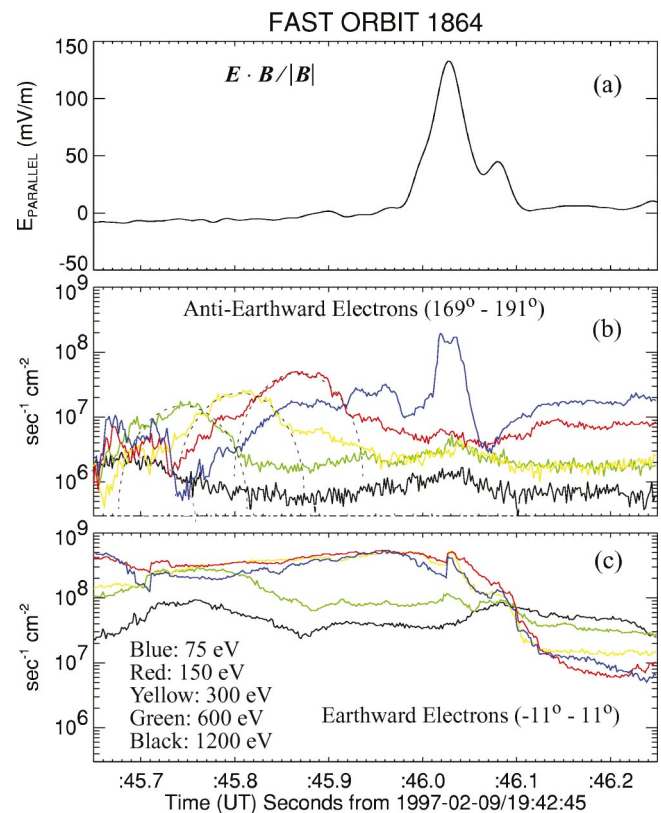


FIG. 2. (Color). A magnified view of the  $E_{\parallel}$  event in Fig. 1. (a)  $E_{\parallel}$  at 200-Hz bandwidth. (b) Anti-earthward ( $168.25^{\circ}$ – $191.25^{\circ}$  in pitch angle) electron energy flux vs time at  $\sim 2$ -ms resolution. The traces represent energy flux in  $\Delta \xi / \xi = 0.15$  energy bands. The colors indicate the center energies as indicated on the plot. (c) Earthward ( $-11.25^{\circ}$ – $-11.25^{\circ}$  in pitch angle) electron energy flux vs time at  $\sim 2$ -ms resolution.

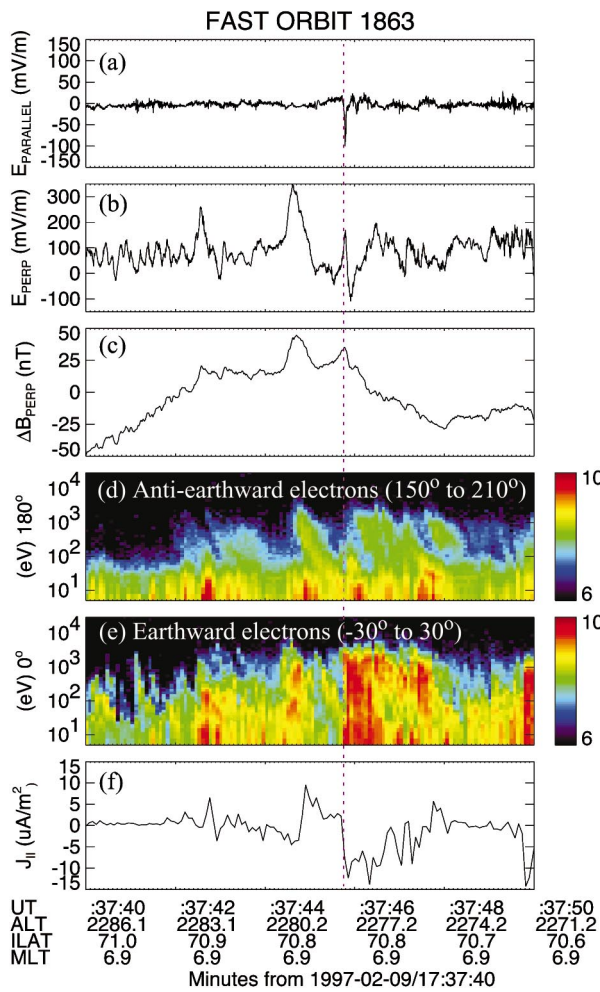


FIG. 3. (Color). Another example of an observation of a large-amplitude parallel electric field associated with an inertial Alfvén wave plotted in the same format as Fig. 1. (a)  $E_{\parallel}$  at 200-Hz bandwidth. (b)  $E_{\perp}$  at 200-Hz bandwidth. The component is closest to the spacecraft velocity. (c)  $\Delta B_{\perp}$ , the measured magnetic field minus the Earth's model field, at  $\sim 5$ -Hz frequency band. (d) Anti-earthward ( $150^{\circ}$ – $210^{\circ}$  in pitch angle) electron energy flux vs energy and time at 79-ms resolution. (e) Earthward ( $-30^{\circ}$ – $30^{\circ}$  in pitch angle) electron energy flux vs energy and time at 79-ms resolution. (f) The field-aligned electron current derived from 5-eV to 30-keV electron fluxes.

Figure 3 displays another event in the same format as in Fig. 1.  $E_{\parallel}$ , plotted in Fig. 3(a), is accurate to approximately  $\pm 25$  mV/m and has a large negative (anti-earthward) peak at  $\sim 17:37:46$  UT.  $E_{\perp}$  and  $\Delta B_{\perp}$  [Figs. 3(b) and 3(c)] have oscillations from  $\sim 1$  to  $\sim 5$  Hz, indicative of an Alfvénic disturbance. As in Fig. 1, field-aligned electron fluxes in both directions display velocity dispersion. The  $E_{\parallel}$  structure in Fig. 3 is coincident with a local maximum in  $\Delta B_{\perp}$  and occurs as the electron fluxes were reversing from anti-earthward to earthward. The field-aligned current, Fig. 3(f), has a sharp change.

The event in Fig. 3 is in many ways similar to the second event in Fig. 1, with an opposite pattern.  $E_{\parallel}$  is upward instead of downward. The event occurs at a local maximum in  $\Delta B_{\perp}$  rather than a local minimum, and the electron fluxes were changing from anti-earthward to earthward instead of earthward to anti-earthward.

Examination of other events shows a similar pattern. The

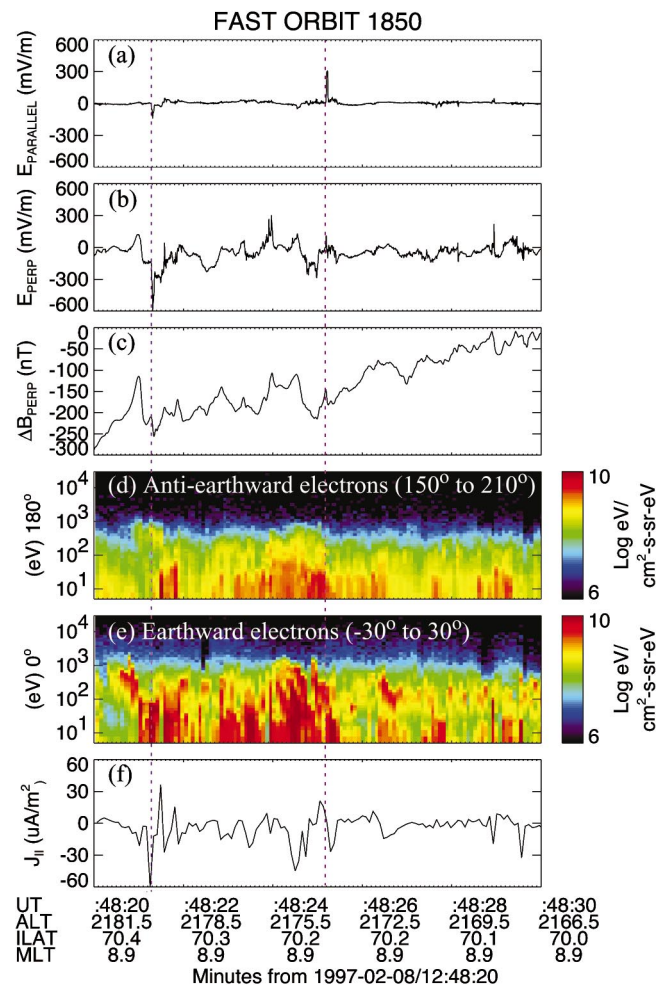


FIG. 4. (Color). Observations of a large-amplitude parallel electric field associated with inertial Alfvén waves during a substorm expansion. Figure 4 is plotted in the same format as Fig. 1. (a)  $E_{\parallel}$  at 200-Hz bandwidth. (b)  $E_{\perp}$  at 200-Hz bandwidth. The component is closest to the spacecraft velocity. (c)  $\Delta B_{\perp}$ , the measured magnetic field minus the Earth's model field, at  $\sim 5$ -Hz frequency band. (d) Anti-earthward ( $150^{\circ}$ – $210^{\circ}$  in pitch angle) electron energy flux vs energy and time at 79-ms resolution. (e) Earthward ( $-30^{\circ}$ – $30^{\circ}$  in pitch angle) electron energy flux vs energy and time at 79-ms resolution. (f) The field-aligned electron current derived from 5-eV to 30-keV electron fluxes.

spiky  $E_{\parallel}$  structures associated with Alfvén wave signatures are almost always associated with a rapid change in electron current (or possibly high-current shear). The direction of the electric field and the sense of the change in current, however, do not appear to be correlated. Figure 4 shows an observation of very strong Alfvén wave activity at the poleward boundary of the auroral zone during a substorm expansion.  $E_{\parallel}$  plotted in Fig. 4(a) is accurate to approximately  $\pm 50$  mV/m. A large-amplitude negative (upward)  $E_{\parallel}$  is seen at  $\sim 12:48:21.3$  UT coincident with a local minimum in  $\Delta B_{\perp}$  and an enhancement in anti-earthward electron fluxes [panel (d)]. A decline in earthward fluxes, Fig. 4(e), is somewhat delayed. The  $E_{\parallel}$  event occurs during a rapid change in field-aligned current.

A large-amplitude positive (downward)  $E_{\parallel}$  is seen at  $\sim 12:48:25.1$  UT coincident with a sharp local maximum in  $\Delta B_{\perp}$ , a decrease in anti-earthward fluxes, Fig. 4(d), and an enhancement in earthward electron fluxes, Fig. 4(e). Once

again, the  $E_{\parallel}$  event occurs during a rapid change in the field-aligned current.

The observations in Fig. 4 show one of the strongest parallel electric fields that have been observed by FAST. The Alfvén wave frequency as seen from the moving spacecraft is  $\sim 1$  Hz, which could indicate  $\sim 6$ -km perpendicular wavelengths if the measured wave frequency is dominated by Doppler shift (the spacecraft is traveling  $\sim 6$  km/s).

### III. DISCUSSION

The observations in Figs. 1, 3, and 4 show large-amplitude, localized parallel electric fields associated with Alfvénic turbulence and accelerated field-aligned electron fluxes. The Alfvénic turbulence is seen to have frequencies from  $\sim 0.5$  to  $\sim 5$  Hz as measured from a moving spacecraft. Often, the short time scale Alfvén waves have a very strong perpendicular electric field, indicating a substantial electrostatic component and short perpendicular scales. The frequency of the Alfvén waves, therefore, could be dominated by Doppler shift. If the signals are dominated by Doppler shift, the wavelengths are on the order of  $\sim 1$  to  $\sim 10$  km, and therefore  $k_{\perp} \delta_e \sim 1$ . These Alfvén waves are in the inertial regime<sup>2-7</sup> and are expected to develop a finite parallel electric field.

Inertial Alfvén waves in the near-earth environment are accompanied by intense, field-aligned electron fluxes<sup>4-7</sup> that often display velocity dispersion. On longer time/perpendicular size scales ( $> \sim 1$  s, 5 km), the electron fluxes are organized by the slope of  $\Delta B_{\perp}$ , whereas on the shorter time/perpendicular size scales ( $< \sim 1$  s, 5 km), the field-aligned electron fluxes are often more intense but not as well correlated with  $\Delta B_{\perp}$ . The dispersion of the electrons is such that field-aligned electron fluxes in both directions can be observed simultaneously as the fluxes are changing direction. In most cases, the fluxes change direction at the local maxima or minima of  $\Delta B_{\perp}$ , where the field-aligned current is expected to be near zero. It is at these regions/times that the parallel electric fields are observed.

#### A. $E_{\parallel}$ structures

In the linear approximation, the amplitude of  $E_{\parallel}$  in an inertial Alfvén wave should be on the order of 0.1 mV/m under the plasma conditions in the examples that we have presented, but the observed amplitudes are roughly 3 orders of magnitude higher. Put another way, the ratio,  $E_{\parallel}/E_{\perp} \equiv k_{\parallel} k_{\perp} / (k_{\perp}^2 + 1/\delta_e^2)$  (e.g., Ref. 6) is  $\sim 10^{-3}$  in linear theory, but is nearly unity in the observations of the spiky structures. These structures are clearly nonlinear phenomena.

A crude estimate of the scale size of the parallel electric fields can be obtained from the speed of the structure (assuming that is along the magnetic field) or from the potential of the structure, which can be roughly established from the perturbations in the electron fluxes. In all the observations presented, the scale sizes of the parallel electric fields are between  $100\lambda_D$  to over  $1000\lambda_D$  (the physical sizes of the structures are several hundred meters, and Debye lengths are on the order of 1 m). These scale sizes differ from those of observed double layers in the downward current region<sup>33,38</sup>

and from theoretical descriptions of double layers (e.g., Refs. 36 and 39), which indicate sizes on the order of  $10\lambda_D$ . Furthermore, the conventional double layer (e.g., Refs. 36 and 39) is expected to occur with a substantial current satisfying the Boehm and Langmuir conditions, whereas the reported  $E_{\parallel}$  structures were at near-zero currents.

The Alfvén wave parallel scale,  $O(10\,000)$  km, and the parallel scale of  $E_{\parallel}$  structures,  $O(1)$  km, are well separated, whereas the perpendicular scale sizes may be nearly identical. Thus, the observed parallel electric fields represent a nonlinear process that couples to substantially different parallel scales.

The lifetimes of  $E_{\parallel}$  structures are not determined, but can be bounded. As a minimum, the lifetime is on the order of the observed duration ( $\sim 50$  ms). As a maximum, the lifetime must be less than the Alfvén period, which varies from  $\sim 0.2$  to  $\sim 2$  s in the observed cases. If the  $E_{\parallel}$  structures are associated with the bidirectional electron fluxes, the overlap between earthward and anti-earthward fluxes ranges is  $O(100)$  ms, only a few times the duration of the observations. The plasma period is on the order of  $\sim 10$   $\mu$ s (Table I), so the above structure formation and decay cover many such periods.

Similar observations have been reported from the Freja satellite.<sup>27</sup> These observations show a possible unipolar  $E_{\parallel}$  fluctuation on the order of 100 mV/m coincident with an Alfvén wave signature that is seen on a much longer time scale in  $E_{\perp}$  and  $\Delta B_{\perp}$ . The  $E_{\parallel}$  fluctuation was observed to be associated with a localized  $\Delta B_{\perp}$  (10 nT) fluctuation. The Freja report<sup>27</sup> suggests that the observed unipolar  $E_{\parallel}$  could be due to double layers or electrostatic shock, but no direct analysis was made to confirm these suggestions. The location of the  $E_{\parallel}$  structures was on the boundary between enhanced earthward and enhanced anti-earthward accelerated electron fluxes. The FAST observations now validate the  $E_{\parallel}$  structures, but do not confirm the localized  $B_{\perp}$  fluctuation. Instead, we report a sharp second derivative in  $\Delta B_{\perp}$ , indicating a rapid reversal (temporal interpretation) in current or strong-current shear (spatial interpretation).

Current-free double layers have been observed in expanding laboratory plasmas.<sup>40-42</sup> These current-free double layers are transient events related to developing plasmas. There has been no generally accepted theoretical analysis of the helicon double layers,<sup>41</sup> so it is not clear if those observed in space have any other similarities.

The observations of the localized parallel electric fields associated with the Alfvénic turbulence are outside the traditional definition of current-carrying double layers that have been observed in space, and thus may represent a new type of electric-field structure or double layer that arises during (or at the boundary of) a strong current reversal. It is also possible that the structures are not time stationary, and thus not suited for the static description of double layers.

#### B. Comparison to theoretical works

A periodic simulation of the nonlinear behavior of the Alfvén wave in a density gradient was performed by Genot *et al.*<sup>24,25</sup> The density gradient causes the Alfvén wave to

rapidly evolve to smaller perpendicular wavelengths. The waves with large  $k_{\perp}$  then developed strong localized  $E_{\parallel}$  structures in response to the accelerated electrons. The  $E_{\parallel}$  structures in the simulation, interpreted as double layers, were  $\sim 30$ – $100$  Debye lengths along  $\mathbf{B}$ , moving slightly faster than the Alfvén wave speed, and had potentials up to 1 kV. A satellite would observe these structures as  $\sim 100$  mV/m fields enduring for  $\sim 2$  ms. In contrast to the observed  $E_{\parallel}$  structures, the  $E_{\parallel}$  structures in the simulation were seen during strong parallel currents, a  $90^{\circ}$  difference in the location in phase with respect to a linear wave seen in  $E_{\perp}$  and  $\Delta B_{\perp}$ . We cannot, at this time, reconcile the observations with the simulations performed by Genot *et al.*<sup>24,25</sup>

The steepening of a wave pulse was analyzed in a kinetic simulation of shear Alfvén waves in homogeneous plasmas.<sup>26</sup> The simulation was from a gyro-averaged kinetic code, which follows the full electron dynamics and takes full account of wave-particle interactions. A localized  $E_{\parallel}$  structure ( $+300$   $\mu$ V/m) formed at the leading edge a unipolar negative wave pulse (accelerating electrons earthward). At the trailing edge of the pulse a broader but still localized weaker  $E_{\parallel}$  structure ( $+50$   $\mu$ V/m) formed. If the simulation was initiated with a bipolar pulse, another narrow  $E_{\parallel}$  structure would be at the trailing edge, creating a double peak signature. The  $E_{\parallel}$  structures in the simulation have some similarities to the observed  $E_{\parallel}$  structures and demonstrate that spiky  $E_{\parallel}$  structures can be created as part of the nonlinear evolution of an Alfvén wave.

### C. Electron acceleration

The linear electron acceleration process by Alfvén waves has been well studied through test particle simulations.<sup>21</sup> These simulations often employ inertial Alfvén waves with very large  $k_{\perp}$  ( $\sim 1$ -km perpendicular wavelengths) and very large  $\Delta \mathbf{B}$  ( $E_{\perp} \sim 1$  V/m) to develop significant parallel electric fields. The parallel electric fields in the simulation are distributed over long distances along  $\mathbf{B}$  and are weak ( $< 1$  mV/m). While such case studies have met with good success, there remain many examples (e.g., Fig. 1 in this paper) in which the linear acceleration process cannot quantitatively account for the intense electron fluxes. None of the linear simulations predict anti-earthward fluxes at the altitude of the FAST satellite ( $\sim 4200$  km).

One strong possibility is that the nonlinear evolution of the Alfvén wave leads to enhanced electron acceleration.<sup>23</sup> A wide variety of nonlinear processes have been predicted by theory and simulation, but it is not known which nonlinear effects dominate and if the dissipation (electron acceleration) is enhanced as a result of the nonlinear behavior.

It is not clear if the observed spiky  $E_{\parallel}$  structures play a significant role in electron acceleration. Since the observed  $E_{\parallel}$  structures appear at near-zero currents, the energy dissipation is expected to be small. The accelerated electron fluxes (Fig. 2) increased with the occurrence of the  $E_{\parallel}$  structure, but rapidly reverted to the previous level as  $E_{\parallel}$  returned to zero. This behavior is in contrast to that of current-carrying double layers in the downward current region<sup>36–38</sup> and implies that the spiky  $E_{\parallel}$  structures associated with

Alfvén waves are transient. The role of spiky  $E_{\parallel}$  structures in electron acceleration is an area of future study.

## IV. CONCLUSIONS

We have presented observations of localized spiky parallel electric fields associated with inertial Alfvén waves and accelerated electron fluxes. The parallel electric fields appear at local maxima or local minima of the  $\Delta B_{\perp}$ , indicating a rapid (or localized) change in the field-aligned current. The net current, however, is near zero. In all of the examples, accelerated electron fluxes with energies many times the ambient plasma temperatures give evidence of an acceleration process and that the electron fluxes are overlapping and in the process of reversing direction.  $\Delta B_{\perp}$  displayed a triangular shape, and  $E_{\perp}$  had a fine structure.

The scale size of the parallel electric-field structures is roughly  $100\lambda_D$  to  $1000\lambda_D$ . The near-zero currents and the large scale size differ from observations in the upward and downward current regions, so the spiky  $E_{\parallel}$  structures do not fit the traditional descriptions of current-carrying double layers, e.g., Refs. 37 and 39. The lifetime of the structures is not established, but can be bounded between  $\sim 50$  ms and  $\sim 2$  s. The observed  $E_{\parallel}$  structures may represent a new class of double layers that are part of a cross-scale coupling process. They appear to be a consequence of the nonlinear evolution of the Alfvén wave and the electron acceleration process.

## ACKNOWLEDGMENTS

This work was supported by NASA Grant No. NAG5-12026, NASA Fast Snapshot Explorer Extended Mission, and NSF Grant No. ATM-0202564.

- <sup>1</sup>A. Hasegawa, *J. Geophys. Res.* **81**, 5083 (1976).
- <sup>2</sup>C. K. Goertz and R. W. Boswell, *J. Geophys. Res.* **84**, 7239 (1979).
- <sup>3</sup>R. L. Lysak and C. W. Carlson, *Geophys. Res. Lett.* **8**, 269 (1981).
- <sup>4</sup>J. E. Wahlund, P. Louarn, T. Chust, H. de Feraudy, A. Roux, B. Holback, P. O. Dovner, and G. Holmgren, *Geophys. Res. Lett.* **21**, 1831 (1994).
- <sup>5</sup>P. Louarn, J. E. Wahlund, T. Chust, H. de Feraudy, A. Roux, B. Holback, P. O. Dovner, A. I. Eriksson, and G. Holmgren, *Geophys. Res. Lett.* **21**, 1847 (1994).
- <sup>6</sup>C. C. Chaston, C. W. Carlson, R. E. Ergun, and J. P. McFadden, *Phys. Scr.*, **T 84**, 64 (2000).
- <sup>7</sup>K. Stasiewicz, P. Bellan, C. Chaston, C. Kletzing, R. Lysak, J. Maggs, O. Pokhotelov, C. Seyler, P. Shukla, L. Stenflo, A. Streltsov, and J.-E. Wahlund, *Space Sci. Rev.* **92**, 423 (2000).
- <sup>8</sup>C. K. Goertz, *J. Geophys. Res.* **85**, 2949 (1980).
- <sup>9</sup>A. N. Wright, *J. Geophys. Res.* **92**, 9963 (1987).
- <sup>10</sup>F. J. Crary, *J. Geophys. Res.* **102**, 37 (1997).
- <sup>11</sup>C. A. Ferraro and C. Plumpton, *Astrophys. J.* **127**, 459 (1958).
- <sup>12</sup>J. V. Hollweg, *J. Geophys. Res.* **104**, 14811 (1999).
- <sup>13</sup>L. C. Jafelice and R. Opher, *Astrophys. Space Sci.* **137**, 303 (1987).
- <sup>14</sup>W. Gekelman, D. Leneman, J. Maggs, and S. Vincena, *Phys. Plasmas* **1**, 3775 (1994).
- <sup>15</sup>C. A. Kletzing, S. R. Bounds, J. Martin-Hiner, W. Gekelman, and C. Mitchell, *Phys. Rev. Lett.* **90**, 035004 (2003).
- <sup>16</sup>R. L. Lysak and W. Lotko, *J. Geophys. Res.* **101**, 5085 (1996).
- <sup>17</sup>A. Keiling, J. R. Wygant, C. Cattell, M. Temerin, F. S. Mozer, C. A. Kletzing, J. Scudder, and C. T. Russell, *Geophys. Res. Lett.* **27**, 3169 (2000).
- <sup>18</sup>C. C. Chaston, W. J. Peria, C. W. Carlson, R. E. Ergun, and J. P. McFadden, *Phys. Chem. Earth* **26**, 201 (2001).
- <sup>19</sup>J. P. McFadden, C. W. Carlson, and R. E. Ergun, *J. Geophys. Res.* **104**, 14453 (1999).
- <sup>20</sup>R. L. Lysak, *J. Geophys. Res.* **93**, 5942 (1988).
- <sup>21</sup>C. C. Chaston, J. W. Bonnell, L. M. Peticolas, C. W. Carlson, R. E. Ergun,

- and J. P. McFadden, *Geophys. Res. Lett.* **29**, 10.1029/2001GL013842 (2002).
- <sup>22</sup>L. Andersson, N. Ivchenko, J. Clemmons, A. A. Namgaladze, B. Gustavsson, J.-E. Wahlund, L. Eliasson, and R. Yu Yurik, *J. Geophys. Res.* **107**, 10.1029/2001JA900096 (2002).
- <sup>23</sup>C.-H. Hui and C. E. Seyler, *J. Geophys. Res.* **97**, 3953 (1992).
- <sup>24</sup>V. Genot, V. P. Louarn, and F. Mottez, *J. Geophys. Res.* **106**, 29633 (2001).
- <sup>25</sup>V. Genot, V. P. Louarn, and F. Mottez, *J. Geophys. Res.* **105**, 27611 (2000).
- <sup>26</sup>C. E. Watt, J. R. Rankin, and R. Marchand, *Phys. Plasmas* **11**, 1277 (2004).
- <sup>27</sup>T. Chust, P. Louarn, M. Volwerk, H. de Feraudy, J.-E. Wahlund, and B. Holback, *J. Geophys. Res.* **103**, 215 (1998).
- <sup>28</sup>K. Stasiewicz, G. Gustaffson, G. Marklund, P. A. Lindqvist, J. H. Clemmons, and L. Zanetti, *J. Geophys. Res.* **102**, 2565 (1997).
- <sup>29</sup>C. C. Chaston, C. W. Carlson, W. J. Peria, R. E. Ergun, and J. P. McFadden, *Geophys. Res. Lett.* **26**, 647 (1999).
- <sup>30</sup>C. W. Carlson, J. P. McFadden, P. Turin, D. W. Curtis, and A. Magoncelli, *Space Sci. Rev.* **98**, 33 (2001).
- <sup>31</sup>R. E. Ergun, C. W. Carlson, F. S. Mozer, G. T. Delory, M. Temerin, J. P. McFadden, D. Pankow, R. Abiad, P. Harvey, R. Wilkes, H. Primsch, R. Elphic, R. Strangeway, R. Pfaff, and C. A. Cattell, *Space Sci. Rev.* **98**, 67 (2001).
- <sup>32</sup>R. C. Elphic, J. D. Means, R. C. Snare, R. J. Strangeway, L. Kepko, and R. E. Ergun, *Space Sci. Rev.* **98**, 151 (2001).
- <sup>33</sup>R. E. Ergun, C. W. Carlson, J. P. McFadden, F. S. Mozer, Y.-J. Su, L. Andersson, D. L. Newman, M. V. Goldman, and R. J. Strangeway, *Phys. Rev. Lett.* **87**, 045003 (2001).
- <sup>34</sup>R. E. Ergun, L. Andersson, D. Main, Y.-J. Su, D. L. Newman, M. V. Goldman, C. W. Carlson, J. P. McFadden, and F. S. Mozer, *Phys. Plasmas* **9**, 3685 (2002).
- <sup>35</sup>F. S. Mozer and C. A. Kletzing, *Geophys. Res. Lett.* **25**, 1629 (1998).
- <sup>36</sup>R. E. Ergun, C. W. Carlson, J. P. McFadden, F. S. Mozer, L. Muschietti, and I. Roth, *Phys. Rev. Lett.* **81**, 826 (1998).
- <sup>37</sup>D. L. Newman, M. V. Goldman, M. Spector, and F. Perez, *Phys. Rev. Lett.* **86**, 1239 (2001).
- <sup>38</sup>L. Andersson, R. E. Ergun, D. Newman, J. P. McFadden, C. W. Carlson, and Y.-J. Su, *Phys. Plasmas* **9**, 3600 (2002).
- <sup>39</sup>L. P. Block, *Cosm. Electrodyn.* **3**, 349 (1972).
- <sup>40</sup>G. Hairapetian and R. L. Stensel, *Phys. Fluids B* **3**, 899 (1991).
- <sup>41</sup>C. Charles and R. W. Boswell, *Phys. Plasmas* **11**, 1706 (2004).
- <sup>42</sup>J. F. Drake, M. Swisdak, C. Cattell, M. A. Shay, B. N. Rogers, and A. Zeiler, *Science* **299**, 873 (2003).